1-1-2015

# Stress and structural damage sensing piezospectroscopic coatings validated with digital image correlation

Gregory Freihofer
*University of Central Florida*

Joshua Dustin

Hong Tat

Axel Schülzgen
*University of Central Florida*

Seetha Raghavan
*University of Central Florida*

Find similar works at: https://stars.library.ucf.edu/facultybib2010

University of Central Florida Libraries http://library.ucf.edu

## Recommended Citation

Freihofer, Gregory; Dustin, Joshua; Tat, Hong; Schülzgen, Axel; and Raghavan, Seetha, "Stress and structural damage sensing piezospectroscopic coatings validated with digital image correlation" (2015). *Faculty Bibliography 2010s*. 6537.
https://stars.library.ucf.edu/facultybib2010/6537

University of
**Central Florida**

✦ **STARS**
Showcase of Text, Archives, Research & Scholarship

# Stress and structural damage sensing piezospectroscopic coatings validated with digital image correlation

Gregory Freihofer [iD], Joshua Dustin [iD], Hong Tat, Axel Schülzgen [iD], and Seetha Raghavan

## ARTICLES YOU MAY BE INTERESTED IN

# Stress and structural damage sensing piezospectroscopic coatings validated with digital image correlation

Gregory Freihofer,[1] Joshua Dustin,[2] Hong Tat,[2] Axel Schülzgen,[3] and Seetha Raghavan[1,a]

[1]*Mechanical and Aerospace Engineering Department, University of Central Florida, Orlando, FL, USA*
[2]*Boeing Research & Technology, Seattle, WA, USA*
[3]*CREOL, The College of Optics and Photonics, University of Central Florida, Orlando, FL, USA*

The piezospectroscopic effect, relating a material's stress state and spectral signature, has recently demonstrated tailorable sensitivity when the photo-luminescent alpha alumina is distributed in nanoparticulate form within a matrix. Here, the stress-sensing behavior of an alumina-epoxy nanoparticle coating, applied to a composite substrate in an open hole tension configuration, is validated with the biaxial strain field concurrently determined through digital image correlation. The coating achieved early detection of composite failure initiation at 77% failure load, and subsequently tracked stress distribution in the immediate vicinity of the crack as it progressed, demonstrating non-invasive stress and damage detection with multi-scale spatial resolution. © *2015 Author(s). All article content, except where otherwise noted, is licensed under a Creative Commons Attribution 3.0 Unported License.* [http://dx.doi.org/10.1063/1.4916760]

The stress dependence of the photo-stimulated luminescence (PL) peaks emitted from $\alpha\text{-}Al_2O_3$ was first used in the form of ruby as a pressure gage in diamond anvil cells,[1] and later found significance as a method to ascertain the stress in the thermally grown oxide of thermal barrier coatings on turbine blades.[2] The shifts that represent the stress-sensitivity of these spectral peaks R1 and R2, known for their high optical efficiency, are material characteristics that have been limited in range to approximately 2.53 $cm^{-1}/GPa$ and 2.54 $cm^{-1}/GPa$ under uniaxial stress respectively.[3,4] Recent work has established the ability to tailor the stress-sensitivity with particle volume fraction when $\alpha\text{-}Al_2O_3$ is deployed as nanoparticles within a matrix.[5] With increasing nanoparticle volume fraction, the PS coefficient was found to increase under applied uniaxial loading to the nanocomposite. For the higher volume fractions, the stress sensitivity increased by nearly 130% with respect to bulk polycrystalline $\alpha\text{-}Al_2O_3$. This prompted the development of these nanocomposites as stress-sensing piezospectroscopic (PS) coatings applied to structural substrates. The potential benefits of high spatial resolution offered by these dispersed nanoparticle sensors range from enabling the qualitative detection of very small stress concentrations such as microcracks or voids to full quantitative stress maps of coated structures to ensure integrity.

To develop the most effective PS nanocoatings, the host matrix for the $Al_2O_3$ nanoparticles should have some degree of transparency, the $Al_2O_3$ nanoparticles should be well dispersed, and the coating should have excellent adhesion to the substrate. The PS nanocoating investigated in this work was manufactured by Elantas PDG, Inc. by mixing 150 nm $\alpha\text{-}Al_2O_3$ nanoparticles (Inframat Corp.) with 99.8% purity in epoxy to achieve a 20% volume fraction of particles. The coating was applied to an Open-hole tension (OHT) composite substrate consisting of laminated IM7-8552 unidirectional tape manufactured and tested in accordance with ASTM standards.[6] Nanoparticle dispersion is of high concern as the nanoparticles have a tendency to agglomerate, thus affecting the load transfer mechanics.[7,8] To inspect the quality of the dispersion, a high resolution PL intensity

---

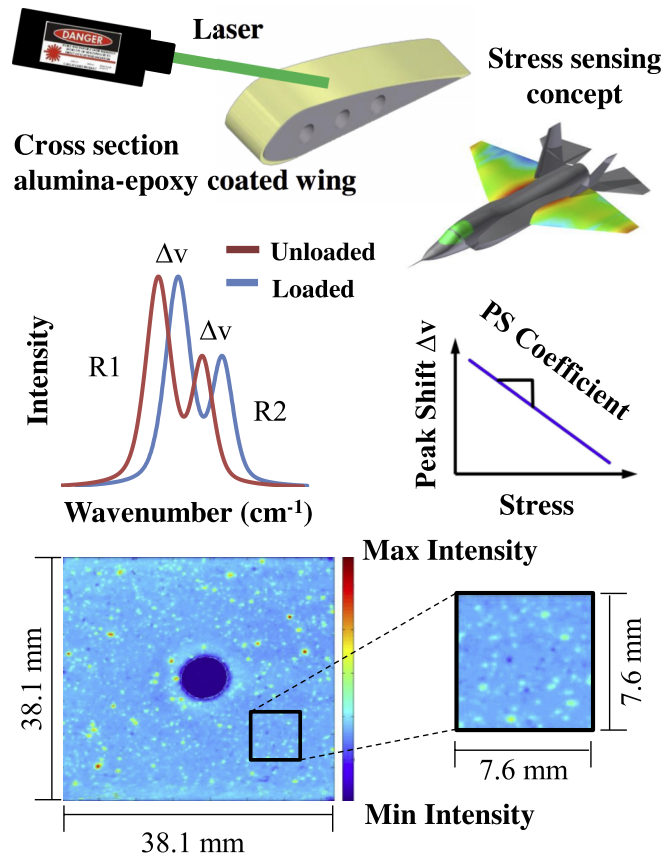[a]Seetha Raghavan: seetha.raghavan@ucf.edu

FIG. 1. Stress sensing concept and theory of piezospectroscopic (PS) nanocoatings. High spatial resolution intensity map quantifies coating dispersion.

map was taken similar to previous work,[9] with a spatial resolution of 70 microns as shown in Figure 1. This map revealed adequate dispersion with the average size of agglomerations in the micron range.

The sample was loaded at a rate of 0.05 in/min and held at discrete increments as shown in Figure 2 using displacement control during holds to maintain constant substrate strain. During each hold, PS and DIC data were collected on the front and back side of the substrate, respectively. PS data were collected with a prototype portable spectrometer system designed to have field capability
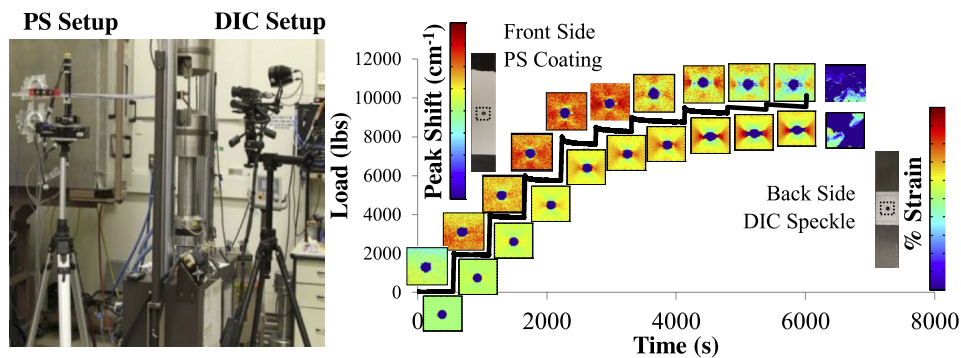


FIG. 2. Experimental configuration of the PS and Digital Image Correlation (DIC) systems about a hydraulic load frame. Front side PL peak shift contours collected at discrete loads are shown above. DIC data were collected on the back side of the composite substrate and are shown below.
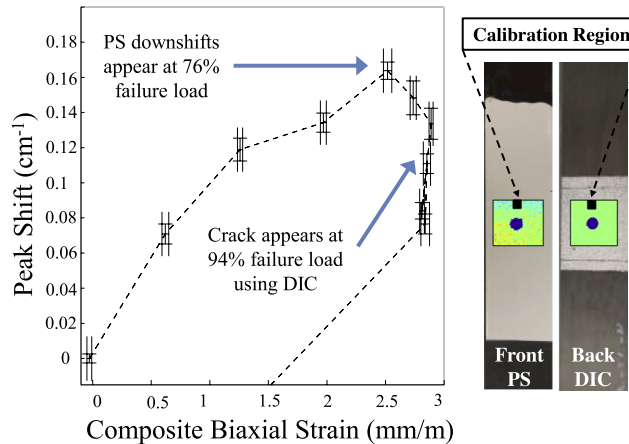
FIG. 3. Early failure detection with the PS nanocoatings. X and Y error bars were equal in size to one standard deviation of the averaged calibration region.

with a 1200 groove/mm grating and a CCD (Princeton Instruments). Excitation was achieved using a low power, 1.5 mW laser of 532 nm wavelength with an exposure time of 100 ms per collection. A back scattering configuration was used with a long working distance objective mounted on an optical probe. The PL spectra, over a measurement area of 25.4 square mm, was implemented using a synchronized translation stage in a 60x60 grid snake scan corresponding to a spatial resolution of 0.4 mm. This spatial resolution can be adjusted to micrometer scales for specific applications.

The R1 peak shift contour maps represent a shift with respect to a baseline wavenumber that was the average of the first map at zero load. These contour maps corresponding to the load-time diagram are shown in Figure 2 using a color scale that identifies positive shifts (upshifts) and negative shifts (downshifts) over the field of view. These plots were compared directly to the strain fields measured by DIC shown below them using a separate color scale that identifies the percentage strain in the region. The qualitative agreement of the DIC measured strain patterns to the PS stress contour maps, as they evolve during the loading cycle, validate the capability of the PS measurements from the nanocoating to capture this evolution. The significance of this result is in the conception of a new non-invasive characterization capability with multi-scale spatial resolution through PS measurements of these nanocoatings.

Although the PS properties are typically correlated to stress,[10] concurrent DIC measurements with PS provides a comprehensive avenue to calibrate the changes in peak position to composite strain. When investigating the PS behavior of this coating, the R1 peak position shift was calibrated with respect to DIC biaxial strain ($\epsilon_x + \epsilon_y$). A region of interest for calibration was chosen furthest away from the hole where the strain field was most uniform as shown in Figure 3. This region of interest was 2 mm x 1.6 mm in size and consisted of 20 PS data points and 72 DIC data points. An average PL peak shift for this region was determined and plotted in Figure 3 with respect to the strain obtained by DIC. The calibration was expected to show a monotonic increase in peak shift as the applied load was increased. This was the case for the first five data points. However, downshifts were observed starting at 77% of failure load. These downshifts correlated closely to the onset of crack formation near the hole. As the PL peak continues to downshift, a maximum biaxial strain is reached just before DIC detects a crack near the open hole at 93% failure load. For the remainder of the test, the PL peak continues to downshift while the biaxial strain remains constant until failure. The PS measurements on the nanocoating demonstrate the capability for early identification of the onset of failure by monitoring the accompanying intrinsic change in load transfer prior to failure detection by DIC.

Gradual downshifts past 77% of the failure load are observed by inspection of the PS contour maps around the hole region shown in Figure 4 and compared with the DIC strain field in this region. Specifically, localized at the open hole edge, there was a greater downshift with respect to the rest of the composite. It is common for OHT composite laminates to begin cracking well
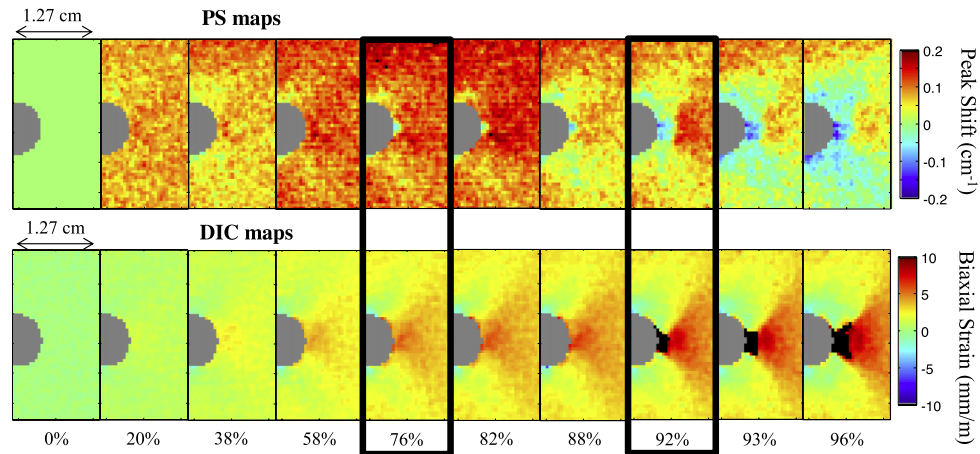
FIG. 4. Crack propagation and failure monitoring of OHT specimen using the PS and DIC method.

before failure.[11] Thus, the downshift close to the open hole may be an indicator of a release in strain energy at the crack tip, while the downshift in the surrounding region potentially indicates an accompanying change in the distribution of stress within the composite. The coating itself was not observed to delaminate from the substrate during the course of loading. The evolution of the peak shift gradients observable in Figure 4 coincides with intrinsic damage patterns of similar composites, including intra-laminate matrix failure in the ±45° plies[12] and initial fiber failure.[13] Near the open hole, DIC cannot measure the strain energy release as it interprets a crack as an unrealistically high strain, which is then filtered from analysis. As shown in Figure 4, PS maps were able to detect the composite damage well before DIC, as illustrated in regions showing a downshift of peak positions near the open hole. In addition, the PL peak drops below the reference position at zero load, indicating a release of residual strain induced on the particles during the coating curing process. This is a benefit for crack and damage detection as the release of residual strain provides an increased contrast in the cracked region. Therefore, PS could serve as an excellent method for failure monitoring, both early detection and at increased loads, through the investigation of strain release in and around the region of a crack.

In conclusion, the demonstration of a PS nanocoating for non-invasive stress sensing of structures was achieved. The potential to monitor real-time stress evolution with high, multi-scale spatial resolution was demonstrated using PS and verified through direct comparison with DIC. The evidence presented here supports that piezospectroscopy can observe propogating damage *via* peak position gradients that enable an attractive damage monitoring technique in structures without the need for a refrence calibration. The integration of additional in-situ characterization with piezospectroscopy, such as X-ray backscatter imaging,[14] could independently verify the correlation between peak shift gradients and subsurface cracking. Many future applications are possible with PS nanocoatings in both laboratory and industrial settings for aerospace, civil applications, and critical load bearing structures in various fields. Future areas of development include high quality PS coatings containing evenly dispersed $\alpha$-$Al_2O_3$ nanoparticles, integration of a full scale PL imaging system with a high powered excitation source while maintaining field mobility, and continued calibration testing for various coating-substrate systems. The extension of this technology for applications in materials research and testing will require multi-disciplinary inputs ranging from nanocomposite manufacturing, novel experimental methods, and calibration testing.

[1] G. J. Piermarini, S. Block, J. D. Barnett, and R. A. Forman, Journal of Applied Physics **46**, 2774 (1975).

[2] A. Selcuk and A. Atkinson, Materials Science and Engineering A **A335**, 147 (2002).

[3] Q. Ma and D. R. Clarke, Journal of the American Ceramic Society **76**, 1433 (1993).

[4] S. Raghavan and P. K. Imbrie, The American Ceramic Society **11**(No. 11), 1 (2009).

[5] A. Stevenson, A. Jones, and S. Raghavan, Nano Letters **11**, 3274 (2011).

[6] ASTM, *D5766/D5766M-11 Standard Test Method for Open-Hole Tensile Strength of Polymer Matrix Composite Laminates*, edited by B. of Standards Volume: 15.03 (ASTM International, West Conshohocken, PA, 2011).

[7] A. S. Jones, G. Freihofer, E. Ergin, K. Lautenslager, W. Gysi, A. Schülzgen, S. Raghavan, and H. Tat, in *Proceeding of the Society for the Advancement of Material and Process Engineering 2012 Conference*, *Baltimore, MD, 21-24 May 2012* (2012).

[8] G. J. Freihofer, S. Frank, E. Ergin, A. S. Jones, A. Stevenson, A. Schülzgen, S. Raghavan, and H. Tat, in *Proceeding of the Society for the Advancement of Material and Process Engineering 2012 Conference*, *Baltimore, MD, 21-24 May 2012* (2012).

[9] A. Stevenson, A. Jones, and S. Raghavan, Polymer **43**, 923 (2011).

[10] H. Tomaszewski, J. Strzeszewski, L. Adamowicz, and V. Sergo, J. Am. Ceram. Soc. **85**, 2855 (2002).

[11] D. R. Hufner and M. L. Accorsi, Composite Structures **89**, 177 (2009).

[12] D. Mollenhauer, E. Iarve, R. Kim, and B. Langley, Composites Part A: Applied Science and Manufacturing **37**, 282 (2006).

[13] P. P. Camanho, P. Maimí, and C. Dávila, Composites Science and Technology **67**, 2715 (2007).

[14] D. Shedlock, T. Edwards, and C. Toh, AIP confrence proceedings **1335**, 509 (2011).